

Numerical Analysis of Shock Oscillation around a Biconvex Circular Arc Airfoil by Incorporating a Bump on it in a Channel

Sujan Barua¹, Sattajit Barua¹, Adibuzzaman Rahi¹, Redowan Ahmed Niloy¹, Shadman Tahmid¹

¹Department of Mechanical Engineering, Bangladesh University of Engineering & Technology

Email:sujanbarua2@gmail.com

Abstract

Oscillatory shock waves are found on airfoils in transonic conditions and are associated with the phenomenon of buffeting, vibration and many other. The present study is mainly devoted to numerical investigation of shock wave characteristics over a 12% biconvex circular arc airfoil in 2D channel by modification of airfoil surface. It was done by installing bump (10% c length and 0.8% c height) on the upper and the lower surface of the airfoil for a specific pressure ratio of 0.71. The bump has been incorporated in such a manner that the mean position of the bump is placed where the RMS of static pressure fluctuation of airfoil surface (for base airfoil) is maximum. Reynolds-averaged Navier-Stokes (RANS) equation with $k-\omega$ SST two equation turbulence model has been applied for computational analysis. The effectiveness of using bump has been analyzed in the present study by investigating flow parameters for different bump heights and a completely new type shock behavior is found for the bump of 0.8% c height.

Keywords: Shock wave, Oscillation, Bump, Transonic

1. Introduction

Shock waves almost inevitably occur in high speed flow around airfoil. This shock wave can be steady or unsteady. The unsteady shock wave strongly interacts with the boundary layer and generate flow instability around the airfoil. This is important in many practical situations in aeronautics, for example in internal aerodynamics such as compressor blade, turbine cascade, nozzle, diffuser, SERP etc. Buffet, high speed impulsive noise, non-synchronous vibration are the detrimental effects caused by the unsteady shock oscillation. Transonic buffet is an extremely strong phenomenon which can cause dangerous vibrations leading to the destruction of a wing or a turbomachine blade.

There have been a great deal of researches on controlling the shock oscillation over decades. Passive control of transonic shockwave/turbulent boundary layer interaction on a porous surface has been experimentally studied by Bahi et al. [1]. Rizwanur et al. [2] investigated shock behavior over supercritical airfoil RAE 2822 with or without shock control cavity. It was observed that the presence of cavity changes the shock behavior from oscillating to steady and the shock strength weakens. Hamid et al. [3] numerically studied the transonic internal flow over a 12% thick symmetric circular arc airfoil and analyzed the various aspects of unsteady flow characteristics in 2014. Based on the geometry of reference [3], Hamid et al. [4] also modified the geometry at $PR=0.69$ and it was observed that the use of cavity totally change the entire flow characteristics and shock properties, which can be used as effective passive control technique to overcome detrimental effect of unsteady shock oscillation. Shock control bump (SCB) is also a passive technique that reduce wave drag in transonic regime. Ashil et al. [5] introduced shock control bump in NLF airfoil. It was observed by Hasan et al. [6] that shock strength in case of bump becomes weak and Root mean square (RMS) of pressure oscillation were reduced significantly compared to no bump model. Mazaheri et al. [7] investigated the interaction of shock and boundary layer around the shock control bump for airfoil RAE-2822 and observed better performance i.e. higher drag reduction, smaller separated areas. Tian et al. [8] investigated the bump crest position, increase of bump height and chord length effect on lift drag ratio at different Mach number. The present study numerically investigates the flow characteristics over a 12% biconvex circular arc airfoil in a two dimensional channel using SCB for pressure ratio of 0.71 and the study also makes comparison between base airfoil and airfoil with bump. Bump of different heights are being investigated and transonic flow behavior for 0.8% c bump height is used in this study. The present investigation find totally different types of shock characteristics including pressure fluctuation, coefficient of pressure due to modification of the geometry with this height of bump.

Nomenclature			
C	chord length(mm)	x	stream wise coordinate(mm)
M	Mach number(-)	y	normal coordinate(mm)
P	pressure (Pa)	C_p	co efficient of pressure(-)
PR	pressure ratio(-)	Subscripts	
Q	dynamic pressure (Pa)	0	total condition
T	time period(s)	b	Back
h_b	Bump height(-)	rms	root mean square

2. Computational domain

The flow is considered as compressible, turbulent and unsteady in our investigation. Density-based solver is used to solve the governing equations of continuity, momentum and energy. As we are dealing with turbulent flows, Reynolds Averaged Navier-Stokes (RANS) equations are used including two additional transport equations of $k-\omega$ SST model. Finite volume method is used to spatially discretize the equations for numerical solution. The base airfoil is identical as reference [3]. Computational domain is shown in Figure 1(a) and close view of base airfoil of with grids is shown in Fig.1.(b). Airfoil with 0.8% c bump with grids and its close view are also shown respectively in Fig. 1(c) and 1(d). Biconvex arc airfoil is used in the present study with chord length, c of 50 mm and maximum thickness is 0.12 c ; leading and trailing edge are kept sharp. Angle of attack is kept at zero degree. Surface modification is done by incorporating bumps, each of length 10% c and heights differing from 3% c , 2% c ,

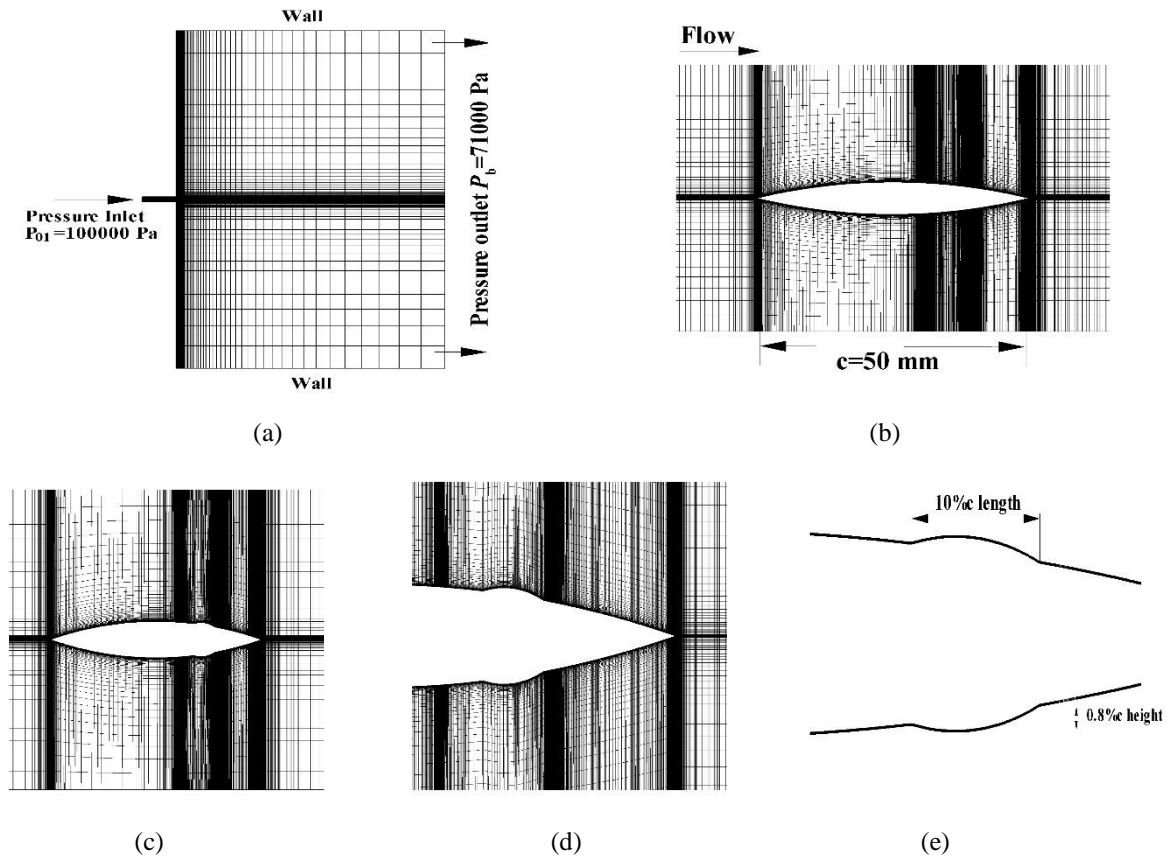


Fig. 1. (a) Computational domain with boundary conditions, (b) Close view of base airfoil with grids, (c) Close view of airfoil with $h_b=0.8\%c$, (d) Zoomed view of the bump, (e) height and width of the bump

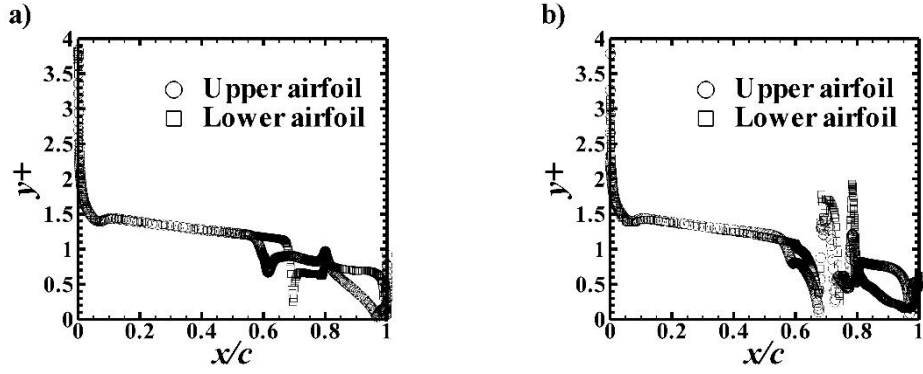


Fig. 2. Distribution of wall y^+ for (a) base airfoil, (b) for airfoil with $h_b=0.8\%c$

$1.5\%c$, $1\%c$ and $0.8\%c$ on both upper and lower surface of airfoil. The mean position of bump is located at $x/c=0.73$ on the airfoil, which shows the peak value for P_{rms} for base case. The origin of (x,y) co-ordinate is located at leading edge of airfoil. Structured mesh is used to discretize the geometry with 93000 grids in case of without bump and 108000 grids in case of with bump model. The minimum normal grid spacing is $5\mu m$. This flow condition creates upstream Mach number of 0.64 of airfoil and the corresponding Reynolds number based on airfoil chord $= 5 \times 10^5$. No slip condition and adiabatic wall condition was applied at solid boundary. Viscosity is considered to be varying with Sutherland's law.

3. Result and Discussion

Lee [9] well explained the mechanism of self-sustained shock oscillation in transonic flows over airfoil, which is known as close feedback loop mechanism. Levy[10] and Yamamoto and Tanida[11] clarified the fundamental mechanism of self-excited shock oscillation. In order to investigate the unsteady shock behavior, a complete cycle of shock oscillation within a time period is shown in a sequential contours of numerically obtained schlieren images at 8 different time steps in Fig. 3. The images show that shock proceeds in both upper and lower surface from downstream to upstream. It is observed that shock appears at one surface after the disappearance of shock at another surface. This confirms the shock behavior to be of Tijdeman type B shock. The transonic flow field becomes modified when a bump is incorporated. Fig.4. shows the computationally obtained schlieren images for a single cycle in case of airfoil with bump. In this case the shock oscillation is also observed but here the shock

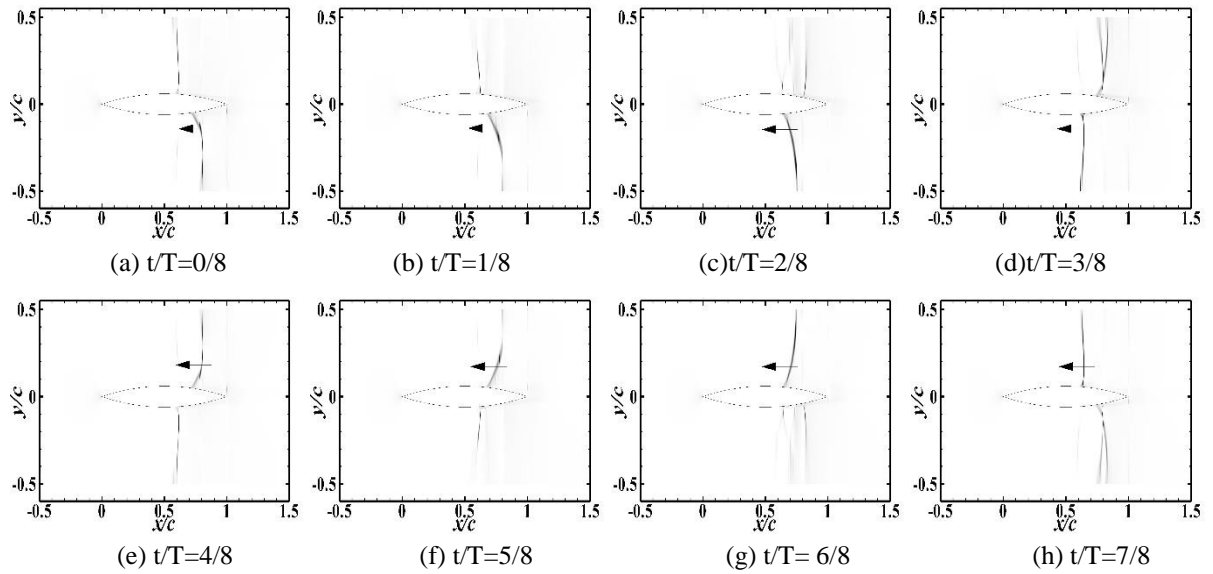


Fig.3. Sequential schlieren images of the flow field in case of base airfoil

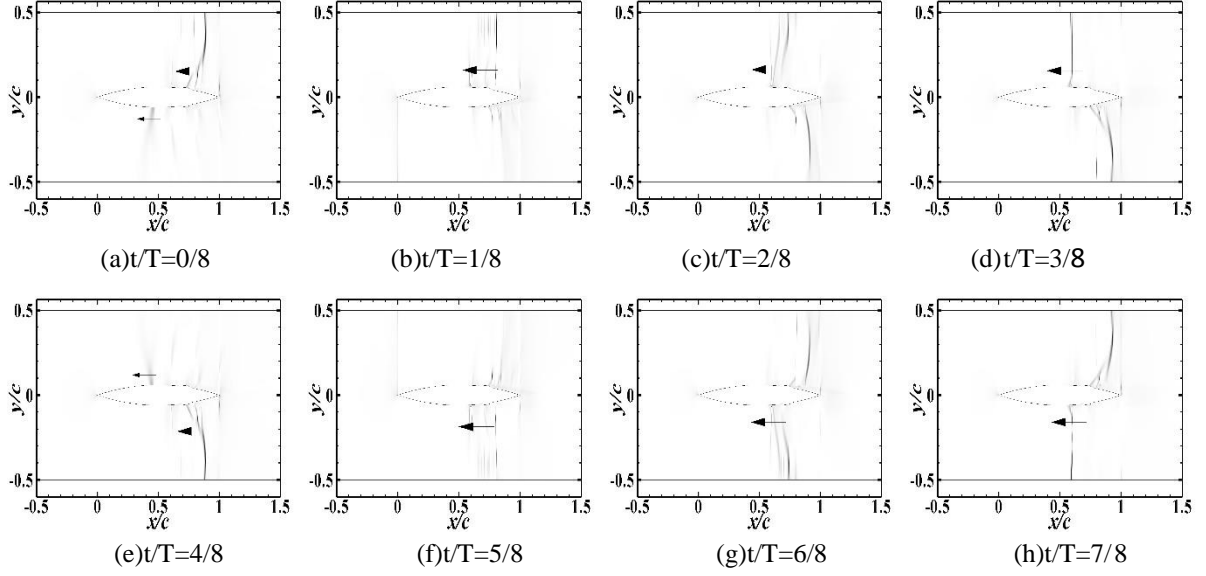


Fig.4. Sequential schlieren images of the flow field in case of airfoil with $h_b=0.8\%c$ bump.

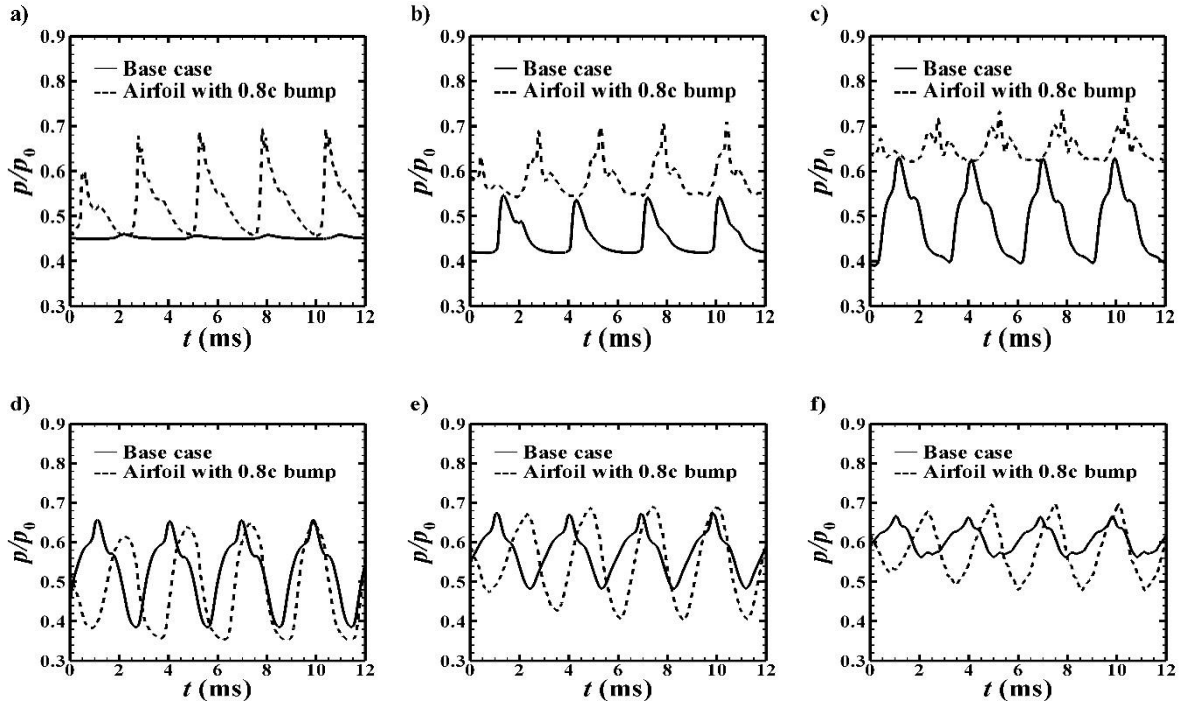


Fig.5. Comparison of static pressure fluctuation of base airfoil and airfoil with bump for (a) $x/c=0.52$; (b) $x/c=0.62$; (c) $x/c=0.68$; (d) $x/c=0.73$; (e) $x/c=0.78$; (f) $x/c=0.84$

propagates along the entire surface of the airfoil. Shock appears at downstream of one surface before fully disappearance of the shock at upstream of another surface.

Fig.5. exhibits the comparison of static pressure fluctuations between the base airfoil and the airfoil incorporating a $h_b=0.8\%c$ bump. It can be seen that unlike the base airfoil, the shock moves entirely on the airfoil surfaces for the case of the airfoil with bump. For the base airfoil, the pressure fluctuation starts from $x/c=0.56$, increases upto $x/c=0.73$ and reaches its maximum value, and then decreases gradually. But for the case of $h_b=0.8\%c$ bump, the pressure fluctuation is present for $x/c=0.56$ in Fig. 5(a). The fluctuation decreases

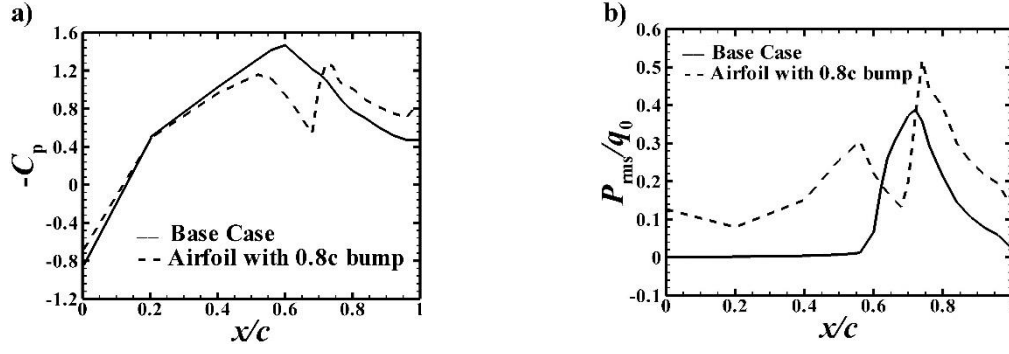


Fig.6. (a) $-C_p$ distribution over upper surface of airfoil; (b) P_{rms}/q_0 distribution for upper surface of airfoil

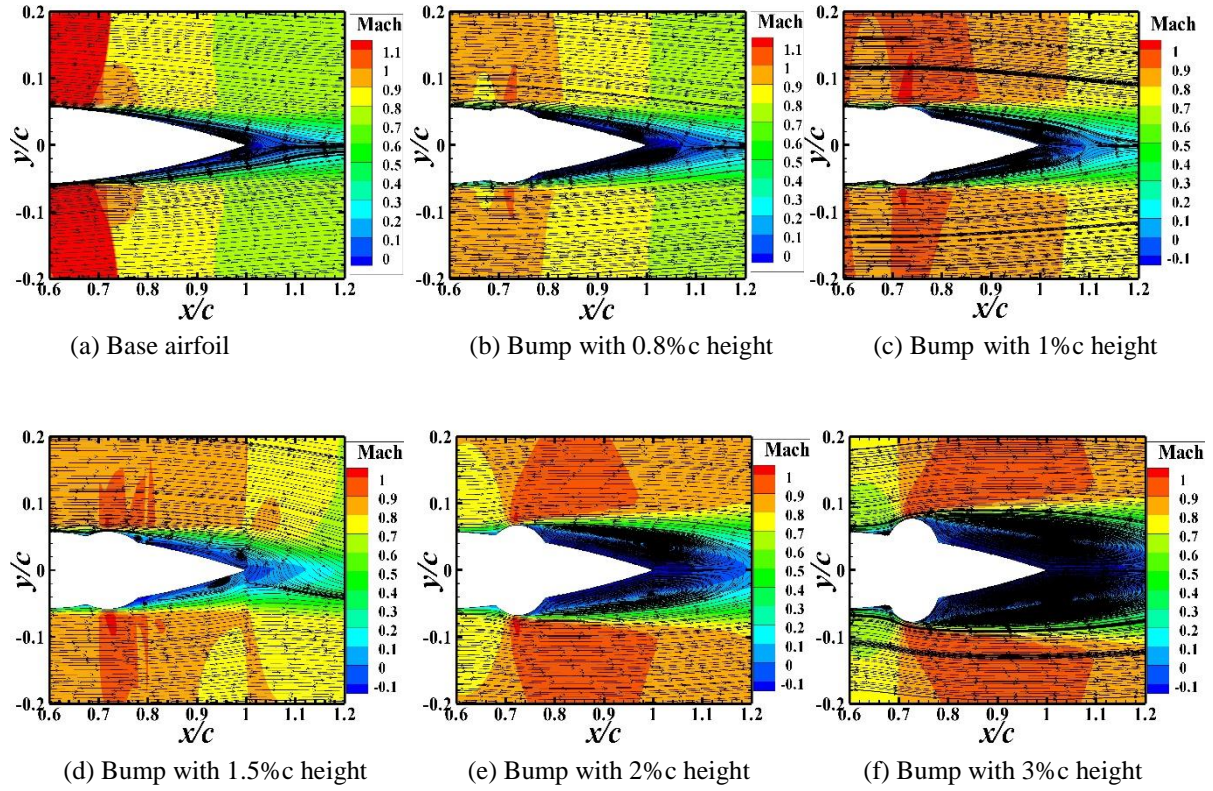


Fig.7. Mach contours for base airfoil and airfoil with bump for different heights.

downstream and at $x/c=0.73$, the fluctuation increases again, and the magnitudes are larger than that of base airfoil, which can be seen in Fig. 5(d), 5(e) and 5(f).

Fig. 6(a) exhibits the $-C_p$ distribution over the airfoil surface. Unlike the base airfoil, the value of $-C_p$ decreases gradually after its peak upto $x/c=0.72$, and a sudden peak occurs at $x/c=0.73$ and decreases gradually. But the overall value of $-C_p$ is significantly lower than that of the base airfoil. Fig. 6(b) shows the root mean

square of the pressure fluctuation, normalized by the free stream dynamic pressure q_0 . The flow field instability can be explained by root mean squared (RMS) value of pressure fluctuation. P_{rms} is calculated as

$$P_{rms} = \sqrt{\frac{\sum_{i=1}^n (P_i - P_{avg})^2}{n}} ; \text{ where } P_{avg} = \frac{\sum_{i=1}^n P_i}{n} \quad (1)$$

Where, P_i =instantaneous static pressure; P_{avg} =mean static pressure; n =number of sample point. Here, for the airfoil with $h_b=0.8\%c$ bump, the value for P_{rms}/q_0 is above 0.1 from the leading edge, and shows two peaks unlike

the single peak of the base airfoil. The first peak is at $x/c=0.56$, which is lower than the peak of the base airfoil, and the second peak is at $x/c=0.73$ (at the peak of the bump), which is significantly higher than that of the base airfoil. It can be seen that the shock propagates over the entire surface of the airfoil, but the mean pressure stays higher than that of the base airfoil.

In present investigation, bump of different heights are incorporated and flow characteristics were being observed. The streamline of the flowfields with Mach contours for different heights of bump is shown in Fig. 7. It shows that, as the height of the bump increases, the flow separation and recirculation of flow increases on the downstream of the bumps, which becomes a key instrument in elimination of shock wave for airfoils with bumps having height greater than 0.8% of chord length. The Mach contours reveal the absence of shock for bump heights larger than $0.8\%c$. For airfoils with bumps higher than $0.8\%c$, a supersonic bubble becomes visible instead of a bow shock. For $h_b=0.8\%c$, the separated flow submerges the bump, thus the shock becoming imminent. But the pressure of the entire region above and below the airfoil stays higher than that for the base airfoil.

4. Conclusion

The present study investigates the flow field characteristics of base airfoil and modified geometry of airfoil with bumps with different height at $PR=0.71$. The result can be summarized as below:

- (a) The installation of bump effects the transonic flow field and pressure fluctuation around the airfoil.
- (b) Behavior of shock propagation changes entirely for the case of the largest bump for which shock becomes present. The shock now moves through the entire surface of the airfoil instead of oscillating over a small region, but the overall higher pressure on the flowfield reduces the risk of low pressure bubble formation over the airfoil.
- (c) Larger bump installation eliminates shock entirely.

The present study was based on the a circular bump, to observe the periodic shock behavior in transonic phenomenon. Better result can be achieved by constructing bumps using different shape functions.

5. Acknowledgement

This study is affiliated with Multiscale Mechanical Modeling and Research Modeling Network (MMMRN).

6. Reference:

- [1] L. Bahi, J.M. Ross, and, H.T. Nagamatsu, "Passive shock wave/boundary layer control for transonic airfoil drag reduction", *Proc. of the AIAA*, 1983.
- [2] M.R. Rahman, M.I. Labib, A.B.M.T. Hasan, M. Ali, Y. Mitsutake, and T. Setoguchi, "Effect of cavity on shock oscillation in transonic flow over RAE2822 supercritical airfoil", *Proc. of the AIP*, Vol.1754, 2016.
- [3] M.A. Hamid, A.B.M.T. Hasan, S.M. Alimuzzaman, S. Matsuo, and T. Setoguchi, "Compressible flow characteristics around a biconvex arc airfoil in a channel", *Propulsion and Power Research*, Vol.3(1), pp. 29-40, 2014.
- [4] M.A. Hamid, and A.B.M.T. Hasan, "Passive control of shock oscillation around a biconvex circular arc airfoil in a channel", *Procidia Engineering, Elsevier*, Vol.105, pp. 375-380, 2015.
- [5] P.R. Ashill, J.L. Fulker, and J.L. Shires, "A novel technique for controlling shock strength of laminar-flow airfoil sections", *Proc. of the 1st European Forum on Laminar Flow Technology, Hamburg*, pp. 175-183, 1992.
- [6] A.B.M.T. Hasan, S. Matsuo, T. Setoguchi and H.D. Kim, "Transonic moist air flow around a circular arc blade with bump", *Journal of Thermal Science*, Vol.18, pp. 325-331, 2009.
- [7] K. Mazaheri, K.C. Kiani, A. Nejati, M. Zeinalpour, and R. Taheri, "Optimization and analysis of shock wave/ boundary layer interaction for drag reduction by shock control bump", *Aerospace Science and Technology*, Vol.42, pp. 196-208, 2015.
- [8] Y. Tian, P. Liu, and P. Feng, "Shock control bump parametric research on supercritical airfoil", *Sci. China Technol. Sci.* 2011.
- [9] B. H. K. Lee, "Self-sustained shock oscillations on airfoils at transonic speeds", *Progress in Aerospace Sciences*, Vol. 37, pp.147-196, 2001.
- [10] L.L. Levy, "Experimental and computational steady and unsteady transonic flows about a thick airfoil", *AIAA Journal*, Vol.16, pp. 564-572, 1978.
- [11] K. Yamamoto, and Y. Tanida, "Self-excited oscillation of transonic flow around an airfoil in two-dimensional channels", *ASME Journal of Turbomachinery*, Vol.112, pp. 723-731, 1990.